Rifaximin prophylaxis causes resistance to the last-resort antibiotic daptomycin

A.M. Turner[1], L. Li[1], I.R. Monk[1], J.Y.H. Lee[1,2], D.J. Ingle[1], S. Duchene[1], N.L. Sherry[1,3,4], T.P. Stinear[1], J.C. Kwong[1,4], C.L. Gorrie[1,3]*, B.P. Howden[1,3,4]*† and G.P. Carter[1]*†

[1]Department of Microbiology & Immunology, The Peter Doherty Institute for Infection and Immunity, The University of Melbourne, Melbourne, VIC, Australia

[2]Department of Infectious Diseases, Monash Health, Clayton, VIC, Australia

[3]Microbiological Diagnostic Unit Public Health Laboratory, Department of Microbiology and Immunology, The University of Melbourne at The Peter Doherty Institute for Infection and Immunity, Melbourne, VIC, Australia

[4]Department of Infectious Diseases, Austin Health, Melbourne, VIC, Australia

*These authors supervised this work equally.

†**Corresponding authors:** glen.carter@unimelb.edu.au, bhowden@unimelb.edu.au

Abstract

Bacterial pathogens such as vancomycin-resistant *Enterococcus faecium* (VREfm) that are resistant to almost all antibiotics are among the top global threats to human health. Daptomycin is a new last-resort antibiotic for VREfm infections with a novel mode-of-action, but for which resistance has surprisingly and alarmingly been widely reported. The causes of such a rapid emergence of resistance to this novel antibiotic have been unclear. Here we show that the use of rifaximin, an unrelated antibiotic used prophylactically to prevent hepatic encephalopathy in liver disease patients, is causing resistance to this last-resort antibiotic in VREfm. We show that mutations within the bacterial RNA polymerase complex confer cross-resistance to both rifaximin and daptomycin. Furthermore, VREfm with these mutations are

spread globally across at least 5 continents and 20 countries, making this a major yet previously unrecognised mechanism of resistance. Until now, rifaximin has been considered 'low-risk' for development of antibiotic resistance. Our study shows this is not the case and that widespread rifaximin use may be compromising the clinical efficacy of daptomycin, one of the major last-resort interventions for multidrug resistant pathogens. These findings demonstrate that unanticipated antibiotic cross-resistance may potentially undermine global strategies designed to preserve the clinical use of last-resort antibiotics.

Main

Antimicrobial resistance (AMR) is one of the greatest public health threats that humanity currently faces, with 1.27 million deaths being directly attributable to bacterial AMR in 2019[1]. The magnitude of this threat is therefore similar to that of malaria (558,000 global deaths in 2019)[2], HIV (690,000 deaths in 2019)[3], and diabetes mellitus (1.5 million deaths in 2019)[4]. Infectious caused by multidrug (MDR) and extensively drug resistant (XDR) pathogens are of particular clinical concern since they are associated with frequent treatment failure and high-rates of morbidity and mortality. The preservation of last-resort antibiotics that can be used to treat these formidable pathogens is of critical importance.

Enterococcus faecium is one such formidable pathogen. It is a commensal of the human gastrointestinal tract that has emerged as a major nosocomial pathogen[5]. The intrinsic antibiotic resistance of hospital-associated clones coupled with their ability to rapidly acquire additional antibiotic resistance genes makes *E. faecium* infections increasingly difficult to treat[6]. In particular, strains resistant to vancomycin, the first-line antibiotic for invasive infections, have emerged and disseminated globally due to the acquisition of transferable *van*

49 resistance genes[7]. Consequently, *E. faecium*, which is one of the ESKAPE pathogens
50 (*Enterococcus faecium*, *Staphylococcus aureus*, *Klebsiella pneumoniae*, *Acinetobacter*
51 *baumannii*, *Pseudomonas aeruginosa*, and *Enterobacter spp*.), has been recognised by the
52 World Health Organization (WHO) as a 'high priority' bacterial pathogen[8].
53
54 The lipopeptide daptomycin is a WHO designated 'last-resort' antibiotic that is used 'off-label'
55 to treat severe vancomycin-resistant *E. faecium* (VREfm) infections[9]. The increasing reports
56 of daptomycin-resistant VREfm are of great clinical concern. The specific risk factors for
57 acquiring a daptomycin-resistant VREfm strain are poorly understood, however, patients with
58 a daptomycin-resistant, bloodstream isolate are generally more likely to have been exposed
59 to daptomycin[10,11]. Daptomycin resistance in clinical strains is commonly associated with the
60 presence of specific mutations in the regulatory system LiaRS and cardiolipin synthase Cls[12–
61 14]. However, many daptomycin-resistant VREfm contain wild-type (WT) *liaRS* and *cls* alleles,
62 indicating other unknown molecular pathways are involved[13,15,16].
63
64 In Australia, high rates (15%) of daptomycin-resistant VREfm were recently reported[17], but
65 the data were not epidemiologically robust and genetic determinants leading to resistance
66 were not defined. Accordingly, we undertook a combined genomic and phenotypic analysis
67 to investigate the daptomycin resistance mechanisms in VREfm. Here we show that
68 daptomycin resistance can emerge *de novo* in VREfm following exposure to rifaximin, a
69 commonly prescribed antibiotic used prophylactically to prevent hepatic encephalopathy[18] in
70 liver disease patients. Further, we show that rifaximin-mediated daptomycin resistance is
71 linked with the presence of novel mutations (G482D, H486Y, and S491F) within the rifampicin-
72 resistance determining region (RRDR) of RpoB. Importantly, patients given rifaximin were

73 significantly more likely to harbour daptomycin-resistant VREfm (that also carried RpoB
74 mutations) than patients who did not receive rifaximin. Finally, we show that the identified
75 RpoB mutations arose within the VREfm population soon after rifaximin was first approved
76 for clinical use and have since become globally established, with three independent VREfm
77 lineages currently circulating within at least 20 countries. Our work has therefore uncovered
78 a major new mechanism of daptomycin resistance in VREfm and identified rifaximin, an
79 antibiotic considered to be low-risk for the emergence of bacterial resistance[19], as an
80 important driver of last-resort antibiotic resistance.
81
82 **Results**
83 **Daptomycin resistance in Australian VREfm is polygenic and does not correlate with known**
84 **resistance determinants.**
85 Daptomycin susceptibility testing was performed on VREfm isolated during two unbiased
86 state-wide 'snapshot' studies undertaken for month-long periods in 2015 (n=294) and 2018
87 (n=423) in Victoria, Australia. The proportion of isolates resistant to daptomycin was 16.6%
88 (n=49) in 2015 and 15.3% (n=65) in 2018. Given the unexpectedly high rate of resistance
89 observed, we expanded the study to include additional VREfm isolated in 2017 (n=108) and
90 2018 (n=173) as part of the 'Controlling Superbugs' flagship study[20,21], with 28.4% (n=80) of
91 these isolates being resistant to daptomycin. Overall, we observed 189 (18.9%) daptomycin-
92 resistant VREfm isolates, indicating a very high prevalence of daptomycin resistance in
93 Victoria, Australia.
94
95 To investigate the relationship between daptomycin-resistant and daptomycin-susceptible
96 VREfm, whole-genome comparisons were made for the 998 study isolates plus two additional

97 finished VREfm genomes (one daptomycin-susceptible and one daptomycin-resistant). A
98 maximum-likelihood phylogeny was inferred from an alignment of 6,574 core genome single
99 nucleotide polymorphisms (SNPs) (Supplementary Figure 1). *In silico* multi-locus sequence
100 typing identified 36 sequence types (STs) within the 1000 isolates; 30 of these STs included at
101 least one of the 189 daptomycin-resistant VREfm. Daptomycin resistance was interspersed
102 throughout the tree (i.e. mostly polyphyletic), with several distinct clades. The largest clade
103 (ST203) of daptomycin-resistant strains, accounted for 42.3% of resistant isolates (n=80 of
104 189) and consisted of a single clone predominant during our sampling timeframe (2015 to
105 2018), suggestive of an expanding daptomycin-resistant lineage. The other predominant STs
106 (ST80, ST796, ST1421, and ST1424) consisted of several groups of resistant isolates that did
107 not cluster based on tree structure. The presence of daptomycin-resistant isolates in distinct
108 genetic backgrounds suggested daptomycin resistance has arisen independently within this
109 VREfm population on multiple occasions.
110
111 Given the high prevalence of daptomycin resistance in Australian VREfm isolates, we sought
112 to determine the genetic determinants leading to resistance. Only seven daptomycin-
113 resistant isolates (3.7%) contained the dual LiaR W73C and LiaS T120A mutations. This finding
114 is of note since current literature suggests these mutations are the most important
115 mechanism of daptomycin resistance in VREfm[9,12,22]. In addition, no daptomycin-resistant
116 isolates contained the H215R or R218Q mutations in Cls or the Q75K mutation in the septum
117 site determining protein (DivIVA), which have all previously been linked with daptomycin
118 resistance in VREfm[23]. The mechanism of daptomycin resistance in the majority (n=182) of
119 our resistant study isolates was therefore left largely unexplained by previously characterised
120 mutations.

121 **The S491F mutation in RpoB is a novel mediator of daptomycin resistance in VREfm.**

122 To identify the mutations associated with daptomycin resistance in our study isolates, we
123 performed a genome-wide association study (GWAS) approach on the collection of 1,000
124 VREfm isolates with known daptomycin MIC (Figure 1A). To account for the clonal population
125 structure of the collection, we first removed non-homoplastic variants from the list of core
126 genome mutations to reduce the data set to variants that were acquired at least twice across
127 the phylogeny. We then applied a linear mixed model using a kinship matrix as a random
128 effect. After correcting for multiple testing, the analysis identified 142 mutations (in 73 genes)
129 significantly ($P < 1x10^{-10}$) associated with daptomycin resistance (as a binary variable with a
130 breakpoint of 8 mg L^{-1}). The top five most significant mutations were (i) I274S in an
131 uncharacterised ABC efflux protein ($P = 7.44x10^{-15}$), (ii) G71S in an uncharacterised permease
132 protein ($P = 7.77x10^{-14}$), (iii) V288L in a mannitol dehydrogenase protein ($P = 6.08x10^{-12}$), (iv)
133 S491F in RpoB, which is the RNA polymerase ß subunit (P=1.57x10^{-13}), and (v) T634K in RpoC,
134 which is the RNA polymerase ß' subunit (P=4.40x10^{-11}).

135

136 Deletion of the genes encoding the ABC efflux protein, permease protein, or mannitol
137 dehydrogenase protein had no impact on daptomycin susceptibility in a clinical daptomycin-
138 susceptible strain of VREfm from the ST796 genetic background. Similarly, introduction of the
139 T634K mutation within RpoC did not lead to increased levels of daptomycin resistance.
140 However, introduction of the S491F substitution within RpoB, resulted in a 4-fold increase in
141 daptomycin MIC, from 2 mg L^{-1} to 8 mg L^{-1}, and a daptomycin-resistant phenotype. Since
142 mutations within *rpoB* have previously been associated with daptomycin resistance in
143 *Staphylococcus aureus*[24,25], we focused further experimental investigations on the RpoB
144 S491F mutation.

145

146 Based on amino acid alignment, the S491F mutation is located within the predicted RRDR of
147 *E. faecium* RpoB, which spans amino acids 467 to 493 (inclusive). The majority of study isolates
148 (n=829, 82.9%) contained a WT RRDR; however, 169 (16.9%) VREfm contained at least one
149 mutation within this region (Figure 1B), with the S491F mutation being the most common
150 (n=105). This was followed by H486Y (n=16), G482D (n=12), G482V (n=10), Q473L (n=6),
151 H486R (n=5), and other uncommon (n=3) mutations.

152

153 **Different mutations within the RRDR of RpoB result in daptomycin resistance in VREfm.**
154 Given the association of the S491F mutation in RpoB with daptomycin resistance, we
155 hypothesised that other mutations within RpoB may also alter daptomycin susceptibility
156 (Figure 1B). In keeping with this hypothesis, we observed a putative correlation between
157 strains carrying individual G482D (n=12) and H486Y (n=16) mutations in RpoB and daptomycin
158 resistance, with 10 daptomycin-resistant isolates containing G482D (83.3% resistant) and 13
159 containing H486Y (81.3% resistant). Clinical isolates containing the G482D, H486Y, or S491F
160 mutations were interspersed throughout the phylogenetic tree and identified in distinct STs,
161 highly suggestive of multiple independent acquisitions (Figure 1C). Ongoing expansion was
162 also observed for one dominant, daptomycin-resistant clone (ST203) containing the S491F
163 mutation throughout the isolate collection period (2015-2018).

164

165 The G482D and H486Y mutations were also located within the predicted RRDR region,
166 suggesting a potential correlation between rifamycin and daptomycin resistance. Therefore,
167 rifampicin susceptibility testing (with rifampicin being a marker of rifamycin resistance[26]) was
168 performed on all clinical VREfm containing a RpoB mutation within the predicted RRDR

169 (n=169). A randomly selected collection (n=169) of isolates containing a WT RpoB RRDR were
170 used as a control group in this analysis. Mutations located within the predicted RRDR
171 correlated with high-level rifampicin resistance (median MIC 256 mg L^{-1}), while control
172 isolates containing the WT region displayed a median MIC of 8 mg L^{-1} (Supplementary Figure
173 2). The correlation between rifampicin and daptomycin resistance in clinical strains containing
174 the G482D, H486Y, and S491F mutations, suggested a novel link between rifamycin and
175 daptomycin resistance in VREfm.
176
177 To confirm the G482D and H486Y mutations in RpoB also led to rifamycin and daptomycin
178 resistance we constructed isogenic mutants carrying these mutations in the same rifamycin-
179 susceptible, daptomycin-susceptible, clinical strain of VREfm (ST796), used to make the S491F
180 RpoB isogenic mutant above. Introduction of the G482D, H486Y, or S491F RpoB mutations
181 resulted in a 7-fold decrease in rifampicin susceptibility compared to the WT strain, leading
182 to high-level rifampicin resistance (>512 mg L^{-1}) (Figure 1D). To confirm the changes in
183 rifampicin susceptibility were due to the introduction of each specific mutation and not
184 unknown secondary mutations, we reverted each RpoB mutation to WT by restoration of the
185 chromosomal allele. Complementation to the WT *rpoB* allele in each of the G482D, H486Y, or
186 S491F mutants resulted in reversion of rifampicin MIC to the WT level (8 mg L^{-1}), indicating
187 the RpoB mutations were responsible for the heightened levels of rifampicin resistance
188 observed (Figure 1D). To then determine if the G482D and H486Y mutations could also cause
189 daptomycin resistance, daptomycin susceptibility testing was performed. Similar to the S491F
190 isogenic strain, introduction of the G482D or H486Y mutation resulted in a 4-fold increase in
191 daptomycin MIC, from 2 mg L^{-1} to 8 mg L^{-1}, and a daptomycin-resistant phenotype (Figure 1E).
192 Complementation with the WT *rpoB* allele onto the chromosome resulted in reversion of

193 daptomycin MIC to the WT level, indicating the G482D, H486Y, and S491F RpoB mutations
194 resulted in cross-resistance to rifamycins and daptomycin in VREfm.
195
196 Given the reported importance of *liaRS* mutations in daptomycin-resistant VREfm, we also
197 introduced the well-characterised LiaR W73C and LiaS T120A mutations into the same clinical
198 strain of VREfm (Figure 1D). No difference in rifampicin MIC was observed after introduction
199 of the *liaRS* mutations, compared to the WT strain, indicating the cross-resistance observed
200 with the G482D, H486Y, and S491F mutations is unique to these RpoB substitutions. However,
201 compared to the WT, introduction of the *liaRS* mutations decreased daptomycin susceptibility
202 2-fold, with a reversion to the WT daptomycin MIC after complementation with the WT *liaRS*
203 alleles. The introduction of the *liaRS* mutations had less of an impact on daptomycin
204 susceptibility than the G482D, H486Y, and S491F RpoB mutations and did not result in a
205 daptomycin-resistant phenotype (MIC $\geq$8 mg L^{-1}). When considered in conjunction with the
206 genomic epidemiology data associated with this study, where *liaRS* mutations were less
207 common than the *rpoB* mutations in daptomycin-resistant VREfm (n=7 versus n=141,
208 respectively), our data suggests that mutations within RpoB might represent a previously
209 uncharacterised, yet important mechanism of daptomycin resistance in VREfm.
210
211 **The G482D, H486Y and S491F RpoB mutations are common in international VREfm strains.**
212 To determine if the *rpoB* mutations associated with daptomycin resistance observed in
213 Australian VREfm were representative of other VREfm isolates globally, we performed a large-
214 scale analysis using publicly available VREfm sequence data from healthcare-associated
215 strains (n=4,476; n=3,476 international and n=1,000 Australian) (Figure 2A). Of the isolates
216 analysed, 630 (14.3%) carried an amino acid substitution in the RRDR of RpoB, occurring at 16

217 positions (Figure 2B). The S491F mutation was the most common, being present in 461
218 isolates, and accounting for 77.9% of the RpoB mutations observed. Isolates carrying this
219 mutation originated from 20 countries, and *in silico* MLST showed the mutations were spread
220 across 21 different STs, with ST203 (44.7%), ST80 (30.2%), and ST117 (11.5%) accounting for
221 the majority (86.4%) of isolates carrying this substitution. Importantly, five VREfm harbouring
222 the S491F mutation also contained the *cfr(B)* (n=4) or *poxtA* (n=1) genes that confer resistance
223 to linezolid, suggesting near pan-resistant strains of VREfm have already emerged.
224
225 The H486Y mutation was the second most common, and was identified in 73 isolates,
226 equivalent to 11.6% of strains with mutations within the RRDR of RpoB. These isolates were
227 collected from 10 countries and *in silico* MLST identified 22 STs, with the most common being
228 ST203 (23.2%), ST796 (21.9%), and ST80 (20.5%). The G482D mutation was the third most
229 common, being identified in 43 isolates, and accounting for 6.8% of strains carrying RpoB
230 mutations. It was present in nine distinct STs, although mostly commonly in ST796 (65.1%)
231 and ST1421 (11.6%), and was identified in isolates from seven countries. Collectively, these
232 data indicated the G482D, H486Y, and S491F mutations, which confer cross-resistance to
233 rifamycins and daptomycin, are not restricted to Australian VREfm but are globally prevalent
234 in healthcare-associated VREfm strains.
235
236 To determine whether the identified RpoB mutations were enriched within healthcare-
237 associated VREfm (established as clade A1), we interrogated publicly available genomic
238 sequences of VREfm from clade A2 (n=98), known for being animal-associated[27]. In keeping
239 with previous findings, the maximum-likelihood tree clustered isolates into two main clades:
240 one healthcare-associated and one associated with VREfm from animals. No mutations were

241 identified in the RpoB RRDR region of strains isolated from animals, with our analyses showing
242 that RRDR RpoB mutations were significantly (P<0.001; Fisher's exact test) associated with
243 healthcare-associated VREfm. This suggests the identified RpoB mutations are primarily
244 enriched within the healthcare setting (Supplementary Figure 3).
245
246 **Phylodynamics indicate the S491F RpoB mutation emerged within the VREfm population**
247 **following the clinical approval of rifaximin.**
248 Given the predominance of the S491F mutation in globally distributed VREfm populations, we
249 used evolutionary phylodynamic analyses to understand its emergence. Within our Australian
250 isolates, we observed the expansion of a dominant ST203 clone from 2015 to 2018 that
251 carried the S491F mutation (Figure 1C). Since this clone comprised VREfm carrying the *vanA*
252 resistance cluster or operon, we sequenced all "historical" *vanA*-VREfm from our public health
253 laboratory (n=229), which consisted of every *vanA*-VREfm isolate collected from 2003 to
254 2014, to increase temporal signal. We then contextualised all Australian isolates (n=1,229)
255 with the international (n=3,389) VREfm in a maximum-likelihood phylogeny inferred from an
256 alignment of 9,277 SNPs and used clustering with core-genome MLST (cgMLST) to identify
257 three clusters containing the RpoB S491F mutation (Figure 3A). The same ST203 clone (Cluster
258 1) formed the largest cluster (n=219 taxa), consisting of isolates from Australia and United
259 Kingdom. Cluster 2 (n=85 taxa) consisted of ST80 and ST78 isolates from Australia, Europe,
260 South America, the United Kingdom, and the United States of America while Cluster 3 (n=68
261 taxa) consisted of ST80 isolates from Australia, Europe, and the United Kingdom.
262
263 To model the evolutionary trajectories of these three VREfm clusters, we used core-genome
264 SNP diversity and year of isolation (Figure 3B). Bayesian phylodynamic analyses were

265 conducted using the core-genome SNP alignments for each cluster/lineage with a discrete
266 trait model and constant coalescent tree prior. We assessed for temporal signal within each
267 cluster using a root-to-tip regression (Supplementary Figure 4). The substitution rate (the
268 number of expected substitutions per site per year) was consistent with other estimates for
269 healthcare-associated VREfm, otherwise referred to as clade A1[27–30]. The median substitution
270 rate was similar for Cluster 1 and Cluster 2, at 9.7×10^{-7} [95% highest posterior density (HPD)
271 $6.88 \times 10^{-7} – 1.24 \times 10^{-6}$] and 1.25×10^{-6} (95% HPD $7.68 \times 10^{-7} – 1.74 \times 10^{-6}$) respectively, but slightly
272 faster for Cluster 3 at 3.86×10^{-6} (95% HPD $2.23 \times 10^{-6} – 5.69 \times 10^{-6}$). The year of emergence for
273 the most recent common ancestor (MRCA) was estimated for each cluster to indicate when
274 the RpoB S491F mutation was first acquired. The MRCAs for the clusters were similar, with
275 2006 (HPD 1993 – 2012) for Cluster 1, 2000 (HPD 1989 – 2008) for Cluster 2, and 2004 (HPD
276 2001 – 2010) for Cluster 3, suggesting the lineages emerged at similar times (Figure 3C).
277
278 Given the association of the S491F mutation in RpoB and rifamycin resistance, we
279 hypothesised rifamycin use might be driving the emergence of this mutation. The most
280 commonly used rifamycin antibiotics in clinical practice are rifampicin and rifaximin. Since
281 rifampicin was approved for clinical use by the United States Federal Drug Administration
282 (FDA) in 1971, several decades before the estimated emergence of the MRCAs, it is unlikely
283 to have played a major role in the emergence of the S491F mutation within this VREfm
284 population. However, the MRCA for all three clusters is predicted to have emerged around
285 the same time as the first clinical introduction of rifaximin, in 2004. The acquisition of the
286 same mutation in three genetically distinct lineages at a similar time, provides support for our
287 hypothesis that rifamycin use might be driving selection of the S491F mutation within VREfm.
288 Further, the structure of the three maximum clade credibility (MCC) trees (Figure 3B)

289 suggested the lineages have expanded over time, which may be correlated with the approval
290 and subsequent widespread, international use of rifaximin for the prevention of hepatic
291 encephalopathy since 2010 (Figure 3B).
292
293 The S491F mutation in Cluster 1 and Cluster 2 was found to be stably maintained within each
294 lineage after its acquisition, with few high probability events of reversion to the WT *rpoB*
295 allele, indicative of maintenance after emergence (Supplementary Figure 5A-B). For Cluster
296 3, the RpoB S491F mutation emerged a single time, with high (~0.95) posterior probability of
297 a single acquisition within the cluster and subsequent maintenance (Supplementary Figure
298 5C). There was also an equal posterior probability of either a second acquisition within the
299 cluster or loss of the RpoB S491F mutation within Cluster 3. Overall, the Markov jumps for all
300 three clusters suggests that the S491F mutation emerged and was then subsequently
301 maintained within these globally prevalent lineages. Taken together these data show the
302 S491F mutation has emerged within the VREfm population on several occasions since the
303 early 2000s, with the predicted dates of emergence being closely correlated with the clinical
304 introduction of rifaximin.
305
306 **Rifaximin drives the emergence of daptomycin-resistant VREfm in a murine model of**
307 **gastrointestinal colonisation.**
308 Rifaximin is a non-absorbable oral agent with direct antimicrobial activity in the
309 gastrointestinal tract. It is predominately used to prevent recurrent hepatic encephalopathy
310 in patients with liver cirrhosis[18,31]. Importantly, this patient cohort is high-risk for VREfm
311 colonisation within the gastrointestinal tract[32]. Since the Bayesian phylodynamic analyses
312 highlighted a putative correlation between the S491F RpoB mutation in VREfm and use of

313 rifaximin, we hypothesised rifaximin use may be driving the emergence of this mutation and
314 therefore, daptomycin-resistant VREfm within the gastrointestinal tract of patients receiving
315 this antibiotic. To test this hypothesis, mice were colonised with a clinical, daptomycin-
316 sensitive (MIC 2 mg L^{-1}) VREfm strain (Aus0233) containing a WT *rpoB* gene before being
317 administered a human-equivalent dose of rifaximin, rifampicin, daptomycin, or vehicle (Figure
318 4A and Supplementary Figure 6). Rifampicin was chosen as a comparison since it is also a
319 commonly used rifamycin in clinical practice. After 7 days of rifamycin treatment, we
320 observed rifamycin-resistant VREfm in significantly more mice receiving rifaximin (90% of
321 mice) or rifampicin (80% of mice) than in mice that received daptomycin (0% of mice) ($P <$
322 0.0001 and $P < 0.0001$; unpaired *t*-test) or vehicle (0% of mice) ($P < 0.0001$ and $P < 0.0001$;
323 unpaired *t*-test) (Figure 4B).
324
325 For each mouse, we then determined the percentage of individual VREfm isolates that were
326 rifamycin-resistant or daptomycin-resistant. There were significantly more rifamycin-
327 resistant VREfm isolated from mice receiving rifaximin or rifampicin than mice receiving the
328 vehicle control ($P < 0.001$ and $P < 0.01$; unpaired *t*-test) or daptomycin ($P < 0.001$ and $P < 0.01$;
329 unpaired *t*-test) (Figure 4D). Similarly, there was significantly more daptomycin-resistant
330 VREfm in mice receiving rifaximin or rifampicin than vehicle control ($P < 0.05$ and $P < 0.05$;
331 unpaired *t*-test) or daptomycin ($P < 0.05$ and $P < 0.05$; unpaired *t*-test) (Figure 4E). We
332 estimated that daptomycin-resistant VREfm accounted for between 0-41% of the
333 gastrointestinal VREfm population in mice given rifaximin and 0-36% in mice given rifampicin,
334 demonstrating conclusively that rifamycin administration can drive the emergence of VREfm
335 with cross-resistance to rifamycins and daptomycin. Notably, no daptomycin-resistant VREfm
336 were isolated from mice receiving daptomycin, in agreement with prior research[33].

337

338 To identify which mutations were present in the rifamycin-resistant VREfm isolates collected
339 from mice administrated either rifaximin or rifampicin, we randomly selected 150 isolates
340 from each antibiotic group (rifaximin or rifampicin, n=300 total) to undergo WGS, consisting
341 of 100 rifamycin-resistant isolates collected following the last day of treatment and 50 isolates
342 from before rifaximin or rifampicin administration. No mutations in RpoB were identified in
343 any VREfm isolate collected prior to rifaximin or rifampicin exposure. However, following the
344 administration of either rifaximin or rifampicin, VREfm carrying mutations within RpoB were
345 commonly identified. The S491F mutation was most abundant (n=53 and 63, respectively),
346 with all isolates carrying this mutation being daptomycin-resistant (Figure 4F). The H486Y
347 mutation was also commonly identified, albeit less so than S491F, (n=12 and 28, respectively),
348 with all isolates again being daptomycin-resistant. The G482D mutation was the third most
349 commonly identified RpoB mutation (n=15 and 6, respectively), with 13 isolates carrying this
350 mutation being daptomycin-resistant. Note that 2 isolates containing the G482D mutation in
351 the rifampicin treated mice were daptomycin-sensitive, likely due to other confounding
352 mutations within the genome. Other RpoB mutations in addition to S491F, H486Y, and G482D
353 were also identified. These included V135F, L471V, E473L, and H486A, however all VREfm
354 isolates carrying these mutations were daptomycin-sensitive. Importantly, the proportions of
355 each RpoB mutation observed in VREfm collected from the gastrointestinal tract of mice
356 administered either rifaximin or rifampicin, correlated closely the proportions of each
357 mutation observed in our collection of human clinical VREfm isolates, with the S491F
358 mutation most commonly identified, followed by H486Y, and then G482D, suggesting a
359 similar selective pressure (i.e. rifamycin use) found in our mouse experiments might be driving
360 the emergence of similar RpoB mutations within human clinical isolates. Taken together,

361 these data demonstrate that exposure to rifaximin can drive the emergence of daptomycin
362 resistance in colonising strains of VREfm, through the enrichment of isolates carrying select
363 mutations in RpoB.
364
365 **VREfm collected from patients receiving rifaximin are more likely to be daptomycin-**
366 **resistant than VREfm collected from patients that did not receive rifaximin.**
367 To further test our hypothesis that rifaximin use might be driving the emergence of
368 daptomycin resistance in VREfm, we performed a case-control analysis of clinical VREfm
369 isolates collected from a retrospective cohort of patients from a single tertiary healthcare
370 centre in Melbourne, Australia over 4 years. The VREfm isolates were stratified according to
371 whether the patient had received rifaximin within 1 month of VREfm isolate collection or not.
372 A total of 50 VREfm strains were identified as being from patients receiving rifaximin. As a
373 control group, we randomly selected 50 VREfm that had been collected from patients that
374 had not received rifaximin. The majority (88%) of these VREfm were screening samples. All
375 isolates were collected over the same time frame and from the same institution.
376
377 A maximum-likelihood phylogeny was inferred from an alignment of 12,430 core-genome
378 SNPs (Figure 5A). The VREfm isolates in the rifaximin and control groups were dispersed
379 throughout the tree, with 5 different STs (ST78, ST80, ST203, ST796, ST1421, and ST1424)
380 from rifaximin patients and 6 different STs (ST17, ST78, ST80, ST203, ST796, ST1421, and
381 ST1424) from the control patients. There were 28 VREfm from the rifaximin group that
382 contained a mutation within the RRDR of RpoB, with 17 containing the S491F mutation, 5
383 G482D, 4 H486Y, 1 E473L, and 1 G482V mutation. All isolates containing the S491F, H486Y,
384 and G482D mutations were resistant to daptomycin, while isolates with the E473L and G482V

385 mutations were daptomycin-susceptible. The control group had 2 isolates with RRDR RpoB
386 mutations, with 1 susceptible isolate containing a D476Y and 1 daptomycin-resistant isolate
387 containing the S491F substitution.
388
389 Rifaximin exposure in patients was significantly correlated with the isolation of a rifamycin-
390 resistant (*P* = 0.00007, OR = 60.0, 95% CI = 8.8 – 2562.1; Fisher's Exact Test) and daptomycin-
391 resistant VREfm strain (*P* = 0.0006, OR = 25.0, 95% CI = 5.5 – 235.3; Fisher's exact test) (Figure
392 5B and C). These data indicated that patients receiving rifaximin are significantly more likely
393 to carry rifamycin-resistant and daptomycin-resistant strains of VREfm than patients who did
394 not receive rifaximin, suggesting rifaximin use might be an important driver in the *de novo*
395 emergence and spread of daptomycin-resistant VREfm.
396
397 **Discussion**
398 In this study we have shown that specific mutations within the RRDR of RpoB represent a new,
399 major mechanism of daptomycin resistance in VREfm. Our analyses demonstrate these
400 mutations are globally distributed within the VREfm population and are as prevalent as other
401 well-characterised mutations within LiaRS and Cls, which have been previously associated
402 with daptomycin resistance in VREfm and assumed to be the dominant mechanisms[22,34,35].
403 Given the similar prevalence, as well as the finding that isogenic mutants carrying the G482D,
404 H486Y or S491F RpoB mutations display a greater level of daptomycin resistance than isogenic
405 strains carrying mutations in LiaRS, the RpoB mutations discovered here add to the list of
406 clinically relevant mutations involved in the emergence of daptomycin-resistant VREfm.
407

408 Our data suggest the S491F substitution is the dominant RRDR RpoB mutation in VREfm and
409 is present in at least three phylogenetically distinct lineages currently circulating within
410 healthcare systems globally, including in Australia, the United Kingdom, the United States of
411 America, and across Europe. The extent of their dissemination is likely to be underestimated
412 in regions with limited representation in our analyses, such as in Asia, Africa, and South
413 America. It is of clinical concern these lineages have successfully spread over geographic
414 scales and persisted for at least 15 years, since it suggests these globally prevalent lineages
415 might eventually compromise the therapeutic value of daptomycin for treating VREfm
416 infections. The Bayesian analyses provide support the S491F mutation emerged after the first
417 introduction of rifaximin for clinical use, for treatment of travellers' diarrhea, with each of the
418 MCC trees suggestive of subsequent population expansion. In 2010, rifaximin was shown to
419 be efficacious for the prevention of recurrent hepatic encephalopathy in patients with chronic
420 liver disease[18] resulting in a marked increase in its clinical use. As this patient cohort is
421 predisposed to gastrointestinal VREfm colonisation, we hypothesise that the use of rifaximin
422 in this cohort has driven the population expansion of the S491F mutation in VREfm over
423 subsequent years. Further, our data suggests rifampicin is not a significant driver of these
424 RpoB mutations since therapeutic use of rifampicin has occurred since the 1970s and the
425 emergence of VREfm containing these mutations is much more recent. However,
426 appropriately controlled clinical cohort studies will be needed to test these hypotheses.
427
428 VREfm isolates carrying the G428D, H486Y and S491F RpoB mutations were resistant to
429 rifamycin antimicrobials, in addition to daptomycin. Mutations within the RRDR of RpoB have
430 been associated with rifamycin resistance in numerous bacterial species[26], with exposure to
431 rifamycins being a well-documented driver in the emergence of rifamycin-resistant clones in

432 *Staphylococcus*[36–38]. In keeping with this observation, our data suggests the clinical use of
433 rifaximin may be responsible for selecting VREfm isolates harbouring mutations within the
434 RRDR of RpoB and therefore, indirectly driving the emergence of daptomycin-resistant
435 VREfm. Three lines of evidence support our hypothesis: (i) Bayesian phylodynamic analyses
436 show the emergence of phylogenetically distinct VREfm lineages carrying the S491F is
437 temporally linked with the clinical approval of rifaximin in the early 2000s, (ii) animal
438 experiments demonstrated the administration of rifaximin to mice colonised with VREfm led
439 to the emergence of VREfm strains within the gastrointestinal tract that carried mutations
440 within RRDR of RpoB and were resistant to rifamycins and daptomycin, and (iii) an analysis of
441 clinical VREfm isolated from humans showed patients receiving rifaximin were significantly
442 more likely to carry VREfm strains harbouring mutations within the RRDR of RpoB that were
443 resistant to both rifamycins and daptomycin, compared to patients that did not receive
444 rifaximin. It is therefore plausible that rifaximin exposure in this patient cohort might be an
445 important factor in the increasing rates of daptomycin-resistant VREfm that are currently
446 being reported[17,39], through the *de novo* emergence of the RpoB mutations and/or ongoing
447 transmission of resistant strains carrying these mutations. Appropriately controlled clinical
448 cohort studies are needed to dissect this hypothesis. Importantly, given the high rates of
449 daptomycin resistance observed, our results suggest daptomycin should not be used for
450 empiric therapy of invasive VREfm infections in patients who are receiving rifaximin.
451
452 Of note is our observation that rifaximin exposure in mice led to the emergence of strains
453 carrying similar RRDR RpoB mutations to those observed in human clinical isolates and the
454 relative abundance of these mutations within isolates collected from the gastrointestinal tract
455 of mice exposed to rifaximin closely resembled the relative abundance of these mutations in

456 our collection of human VREfm, with S491F, G482D and H486Y being the most abundant
457 mutations in both cases. These observations are suggestive of similar selective pressures,
458 such as rifaximin exposure, being at play in both the controlled mouse experiments of our
459 study and in the human population.
460
461 Overall, this research highlights the potentially serious collateral damage that can arise
462 following the introduction of new clinical antibiotic regimens. While the emergence of within-
463 family antibiotic resistance resulting from prophylactic antibiotic use has been described
464 previously[40,41], there are relatively few studies[37] suggesting that prophylactic antibiotics, such
465 as rifaximin, can lead to cross-resistance between unrelated and last-resort antibiotics, as
466 shown here. Careful consideration should therefore be given to the potential impact of
467 prophylactic antibiotics on antimicrobial stewardship practices. Current thinking[42]
468 recommends withholding the use of last-resort antibiotics to limit the emergence and spread
469 of resistance. However, our findings suggest this is not always the case, since gastrointestinal
470 rifaximin exposure can lead to the emergence of daptomycin-resistant VREfm in the absence
471 of daptomycin. Appropriate surveillance for patients colonised in the gastrointestinal tract
472 with nosocomial pathogens and receiving antibiotic treatment for secondary or unrelated
473 conditions is therefore of critical importance in limiting the emergence and spread of new
474 and increasingly antibiotic-resistant clones within the hospital environment.
475
476 In conclusion, we have identified a new, globally important mechanism of last-resort
477 antibiotic resistance in VREfm and show that prophylactic rifaximin use is a likely driver of this
478 resistance. These findings demonstrate the ease with which new antibiotic treatment
479 regiments can drive the emergence of novel multidrug resistant pathogens and highlight the

480 negative impact that unanticipated antibiotic cross-resistance can have on antibiotic
481 stewardship efforts designed to preserve the use of last-resort antibiotics. We advocate for
482 the judicious use of all antibiotics.
483

484 **Methods**

485 **Media and reagents**

486 *E. faecium* was routinely cultured at 37°C in brain heart infusion (BHI) broth (Becton Dickson)
487 or BHI agar (BHIA), BHI solidified with 1.5% agar (Becto Dickson). For electroporation, *E.*
488 *faecium* was cultured in BHI supplemented with 3% glycine and 200 mM sucrose (pH 7.0).
489 *Escherichia coli* was cultured in Luria broth (LB). Broth microdilution (BMD) MICs were
490 performed in cation-adjusted Mueller Hinton with TES broth (CAMHBT) broth (Thermo
491 Fisher). A concentration of 10 mg L^{-1} chloramphenicol (Sigma Aldrich) was used for plasmid
492 selection in *E. faecium* and *E. coli*. The following antibiotics were used at variable
493 concentrations for susceptibility testing: rifampicin (Sigma Aldrich), rifaximin (Sigma Aldrich),
494 and daptomycin (Cubicin).

495 Oligonucleotides were purchased from Integrated DNA Technologies and are listed in
496 Supplementary Table 1. Plasmids were purified with Monarch Plasmid Miniprep Kit (NEB).
497 PCR products and gel extractions were purified using Monarch DNA Gel Extraction Kit (NEB).
498 Genomic DNA was purified using the Monarch Genomic DNA Purification Kit (NEB). Phusion
499 and Phire DNA polymerase was purchased from New England Biolabs.

500 **Bacterial isolates**

501 Bacterial strains used in this study are listed in Supplementary Table 2. Australian bacterial
502 strains were collected across three data projects in the Microbiological Diagnostic Unit Public
503 Health Laboratory (MDU PHL). Two unbiased cross-sectional surveys of VREfm were
504 conducted between 10 November and 9 December 2015 (n=331)[43] and between 1 November
505 and 30 November 2018 (n=323) in the State of Victoria (referred to as the 2015 and 2018
506 Snapshot). During this period, all VREfm-positive isolates (including screening and clinical
507 samples) collected by laboratories across the state were sent to the MDU PHL. In addition,

508 this project included *vanA*-VREfm collected from the "Controlling Superbugs" study[20], a 15-
509 month (April-June 2017 and October 2017-2018) prospective study including eight hospital
510 sites across four hospital networks, resulting in 346 VREfm isolates (308 patients) sent for
511 WGS at MDU PHL. The VREfm were isolated from patient samples (including screening and
512 clinical samples) routinely collected from hospital inpatients. For the 'historical *vanA*-VREfm,'
513 every *vanA* isolate collected within MDU PHL was included. This resulted in an additional 225
514 isolates, sampled between 2008 and 2014.
515 For publicly available isolates, our aim was to capture the diversity of *E. faecium* circulating
516 globally by including isolates that formed part of several key studies involving hospital-
517 associated VREfm (as of January 2021). To be included, isolates needed to have short-read
518 data available, with geographic location (by country), year of collection, and source (human
519 or animal). Reads were only included if they had a sequencing depth of >50x. To capture the
520 diversity of VREfm circulating in the United States, isolates from human sources were
521 downloaded from the PathoSystems Resource Integration Center[44]. All isolates were
522 confirmed to be *E. faecium* with the Kraken2 database (v.2.1.2)[45]. The final number of
523 international isolates compromised those from Africa (n=8), Asia (n=25), Europe (n=2941),
524 North America (n=424), and South America (n=78) (Supplementary Table 2).
525 **Antibiotic susceptibility testing**
526 Daptomycin susceptibility testing was performed using the BMD MIC method as according to
527 CLSI guidelines. In a 96-well plate, a two-fold dilution series (from 32 to 0.5 mg L^{-1}) of
528 daptomycin was made in 100 μL volumes of CAMHBT, additionally supplemented with 50 mg
529 L^{-1} Ca^{2+}. An inoculum of 100 μL *E. faecium* broth culture adjusted to 1 x 10^6 CFU mL^{-1} in
530 CAMHBT was then added to each well. After 24 hours incubation, the MIC was defined as the
531 lowest antimicrobial concentration that inhibited visible growth. All assays were performed

532 in biological triplicate, with the median MIC reported. In accordance with recent guidelines[46],
533 isolates with a daptomycin MIC ≥ 8 mg L^{-1} were considered to be daptomycin-resistant. A
534 daptomycin-sensitive strain (AUS0085)[47] and a daptomycin-resistant strain (DMG1700661)[17]
535 were used as a control.
536 Rifampicin susceptibility testing was performed using the BMD method in CAMHBT. High-
537 level rifampicin resistance was defined with a MIC > 32 mg L^{-1}. All susceptibility testing was
538 performed in triplicate.

539 **Whole-genome sequencing**

540 Genomic DNA was extracted from a single colony using a JANUS automated workstation
541 (PerkinElmer) and Chemagic magnetic bead technology (PerkinElmer). Genomic DNA libraries
542 were prepared using the Nextera XT kit according to manufacturer's instructions (Illumina,
543 San Diego, CA, USA). Whole-genome sequencing was performed using Illumina NextSeq
544 platform, generating 150 bp paired-end reads.
545 The short reads of isolates sequenced at MDU-PHL are available on the NCBI Sequence Read
546 Archive [BioProjects PRJNA565795 (Controlling Superbugs), PRJNA433676 (2015 Snapshot)
547 and PRJNA856406 (2018 Snapshot), and PRJNA856406 (historical *vanA* isolates)].

548 **Phylogenetic analysis**

549 De novo assemblies of the genomes were constructed using Spades[48] (v3.13). In silico MLST
550 were determined using the program mlst with the efaecium database
551 (https://github.com/tseemann/mlst). The 1000 Australian genomes as well as the 4,612
552 Australian and international VREfm were mapped to the reference *E. faecium* genome
553 AUS0085 isolated from a human bacteraemia infection in Victoria, Australia (NCBI accession:
554 CP006620)[47] using snippy (https://github.com/tseemann/snippy) (v4.4.5), applying a minfrac
555 value of 10 and mincov value of 0.9. This reference was selected as it was a publicly available

556 complete genome collected locally and daptomycin-sensitive. A maximum likelihood
557 phylogenetic tree was inferred using IQ-TREE (v2.1.2) with a general time-reversible (GTR +
558 G4) substitution model, including invariable sites as a constant pattern and 1000 bootstrap
559 replicates. Recombination masking was not performed for species maximum likelihood trees
560 due to the small size of the resulting core alignment. All trees were mid-point rooted and
561 visualised in R (v4.0.3, https://www.r-project.org/) using phangorn[49] (v2.5.5), ape[50] (v5.4),
562 ggtree[51] (v2.3.4), and ggplot (v3.3.2).
563 The genome assemblies of all isolates were screened for acquired antimicrobial resistance
564 determinants using abriTAMR (https://github.com/MDU-PHL/abritamr).

565 **Genome-wide association study of daptomycin resistance**

566 A GWAS approach was applied to identify genetic variants of daptomycin resistance in *E.*
567 *faecium*. A genotype matrix of SNPs was constructed and used as input to homoplasyFinder[52]
568 (v0.0.0.9) to determine the consistency index at each locus and kept mutations that had an
569 index of ≤0.5 (indicating at least two independent acquisitions across the phylogeny). We then
570 ran GWAS using daptomycin resistance as a binary trait, where isolates were categorised as
571 resistant if their daptomycin MIC was ≥8 mg L^{-1}. To correct for population structure, we used
572 the factored spectrally transformed linear mixed models (FaST-LMM) implemented in
573 pyseer[53] (v.1.3.6), which computes a kinship matrix based on the core genome SNPs as a
574 random effect. The Bonferroni method was used to correct *P* values for multiple testing.

575 **Core genome MLST (cgMLST) and clustering**

576 cgMLST alleles for each isolate was defined using the public *E. faecium* cgMLST scheme[54] and
577 chewBBACA (v2.0.16), implemented locally in the COREugate pipeline (v2.0.4)
578 (https://github.com/kristyhoran/Coreugate). The pipeline determines the alleles of each core
579 gene for every isolate as defined by the specific pathogen scheme. The *E. faecium* cgMLST

580 scheme contains 1,423 genes. The number of allelic differences between each isolate within
581 this core set of genes is then determined. The cgMLST clusters were determined using single
582 linkage clustering and a pairwise allelic difference threshold of ≤250. This threshold was
583 chosen since it maximised diversity within clusters, to improve temporal sampling depth,
584 while still clustering based on maximum-likelihood tree structure.

585 **Phylodynamic analyses of the emergence of the S491F RpoB mutation in VREfm lineages**

586 To investigate the emergence of the S491F mutation in RpoB in three different lineages, as
587 defined with cgMLST, we undertook further analysis on these clusters/lineages. From the
588 species-level maximum-likelihood tree (Figure 3A), three lineages/clusters were identifiable
589 by cgMLST due to their size (n>50) and presence of the S491F mutation. The three clusters
590 were analysed independently, such that individual core-genome SNP alignments were
591 generated, since this increased the length of the core alignment and number of sites
592 considered. Snippy (https://github.com/tseemann/snippy) (v4.4.5) was used to generate the
593 alignments for each cluster to the corresponding reference genome (AUSMDU00004024 for
594 cluster 1, AUSMDU00004055 for cluster 2, and AUSMDU00004142 for cluster 3). Each core
595 alignment used a within 'cluster reference' (complete genome of the same cluster) to
596 maximise core-SNP alignment length. The reference for each cluster was chosen since they
597 were a locally-collected, closed genome. Recombination was removed from the final
598 alignment using Gubbins[55] (v.2.4.1) to ensure modelling was only informed by SNPs with tree-
599 like evolution within the core genome. Maximum-likelihood trees for each of the three
600 clusters were inferred from the core-SNP alignments [Cluster 1: (n=219 taxa) 329 SNPs;
601 Cluster 2: (n=85 taxa) 541 SNPs; Cluster 3: (n=68 taxa) 764 SNPs] with IQ-tree (v2.1.2)[56] with
602 a general time-reversible (GTR+Γ) substitution model, including invariable sites as a constant

603 pattern. Phylogenetic uncertainty was determined through 1000 nonparametric bootstrap
604 replicates.

605 To investigate temporal signal in the three clusters of VREfm genomes, we first used
606 TempEst[57] (v1.5). A root-to-tip regression analysis was performed on the root-to-tip branch
607 distances within the three, cluster maximum-likelihood phylogenies as a function of year of
608 collection, with the position of the root optimised according to the heuristic residual mean
609 squared method.

610 The frequency of the emergence of the *rpoB* mutation in VREfm was inferred using a
611 discrete trait model implemented in BEAST[58] (v1.10.4). Under this model the SNP alignments
612 are used to infer the evolutionary process (i.e. phylogenetic tree, time, and nucleotide
613 substitution model parameters) for the three clusters. The alignments all shared the HKY
614 substitution model with a gamma distribution for among-site rate variation, and a constant-
615 size coalescent population prior[28]. To avoid ascertainment bias due to using a SNP alignment,
616 the number of constant sites were taken into account for the likelihood calculations. The
617 molecular clock was a relaxed clock with an underlying lognormal distribution. The molecular
618 clock was calibrated using isolation dates for each genome by year of collection and the mean
619 clock rate is shared between all three alignments, but the model allows for the individual
620 alignments to have different standard deviations of the lognormal distribution and also
621 different branch rates. The mean molecular clock rate requires an explicit prior distribution,
622 for which we used a Γ distribution and a 0.95 quantile range of 4.9×10^{-6} and 1.1×10^{-4}
623 substitutions/site/year. This informative prior means that it acts as an additional source of
624 molecular clock calibration that can drive estimates, even in the absence of temporal signal.

625 The presence or absence of the S491F mutation in *rpoB* was used as a binary trait[59,60].
626 The trait model was shared between the three alignments, with the different Markov jumps

627 and rewards (ie changes of trait state and time spent in each state, respectively) recorded for
628 each of the three alignments. The posterior distribution of model parameters was sampled
629 using a Markov chain Monte Carlo of 100,000,000 iterations, sampling every 100,000
630 iterations. Two independent runs were run for the models. We assessed sufficient sampling
631 from the stationary distributions by verifying the effective sample size of key parameters was
632 around or above 200. The final maximum-clade credibility (MCC) trees were visualised in R
633 (v4.0.3, https://www.r-project.org/) using ggtree[51] (v2.3.4). The Markov jumps for the *rpoB*
634 trait for each alignment were visualised in R (v4.0.3, https://www.r-project.org/).

635 **Reconstruction of clinical mutations by allelic exchange**

636 The *liaR*^{W73C}, *liaS*^{T120A}, *rpoC*^{T634K}, *rpoB*^{G482D}, *rpoB*^{H486Y}, or *rpoB*^{S491F} mutations were recombined
637 into the chromosomal copy of each gene in ST796 VREfm (Ef_aus0233) by allelic exchange.
638 The *liaR*^{W73C} and *liaS*^{T120A} mutations were first introduced individually, then together. The
639 region encompassing each gene was amplified by SOE-PCR and recombined into pIMAY-Z[61]
640 by the seamless ligation cloning extract (SLiCE)[62] method and transformed into *Escherichia*
641 *coli* IM08B[61]. The construct was transformed into electrocompetent VREfm[62], with allelic
642 exchange performed as described previously[63]. Allelic exchange was performed as
643 described[63]. Reversion of *liaR*^{W73C} and *liaS*^{T120A}, *rpoB*^{G482D}, *rpoB*^{H486Y}, or *rpoB*^{S491F} mutations
644 were completed using allelic exchange with a construct containing the respective wild-type
645 allele. To delete the ABC transporter protein (EFAU085_02633), permease protein
646 (EFAU02892), or mannitol dehydrogenase (EFAU02627) from the chromosome, deletion
647 constructs were PCR-amplified from Ef_aus0233 genomic DNA and allelic exchange
648 performed as described above. Genome sequencing and analysis of all mutants was
649 conducted as described, with resulting reads mapped to the Ef_aus0233 reference genome
650 and mutations identified using Snippy (https://github.com/tseemann/snippy) (v4.4.5).

651 **VREfm *in vivo* gastrointestinal colonisation experiments**

652 Female C57BL/6 mice at 6-8 weeks of age were purchased from WEHI and maintained in a
653 specific-pathogen-free facility at the Peter Doherty Institute for Infection and Immunity. All
654 animal handling and procedures were performed in a biosafety class 2 cabinet. Animal
655 procedures were performed in compliance with the University of Melbourne guidelines and
656 approved by the University's Animal Ethics Committee

657 The dose for each antibiotic was calculated using the FDA human conversion formula to
658 ensure each mouse was given a human-equivalent dose[64]. To establish gastrointestinal
659 colonisation of VREfm, mice were administered ceftriaxone (410 mg kg^{-1} day^{-1}; AFT
660 Pharmaceuticals) via subcutaneous injection once daily for 7 days, followed by an antibiotic
661 wean period of 24 hours. Mice were then inoculated with 10^6 VREfm in 100 μl PBS by oral
662 gavage. Three days after VREfm inoculation, single-housed mice were administered either
663 rifaximin (113 mg kg^{-1} administered twice daily; Sigma Aldrich), rifampicin (123 mg kg^{-1}
664 administered once day; Sigma Aldrich), or vehicle (Corn oil with 10% DMSO) via oral gavage;
665 or daptomycin (50 mg kg^{-1} administered once daily; Cubicin) via subcutaneous injection [this
666 results in similar exposure (AUC_{0-24}) to that observed in humans receiving 8 mg kg^{-1} of
667 intravenous daptomycin[65]]. The above antibiotic dosing protocol was followed for 7 days.
668 Faecal samples were collected at specific time points throughout the experiment to
669 determine VREfm gut colonisation and for downstream rifamycin and daptomycin resistance
670 analysis. Faecal samples were resuspended in PBS to a normalised concentration (100 mg ml^{-}
671 ^{1}). Serial dilutions were performed, and samples were plated onto Brilliance VRE agar (Oxiod)
672 for VREfm CFU enumeration.

673 For rifamycin and daptomycin analysis, VREfm colonies (n=50 per mouse) from the Brilliance
674 VRE agar plates were replica plated onto BHIA with and without rifampicin 20 mg mL^{-1} to

675 determine the proportion of rifampicin-resistant VREfm in each mouse. All colonies (n=50 per
676 mouse) were then screened for daptomycin resistance using a daptomycin screen. Of which,
677 a single colony was resuspended in PBS, then diluted 1/100 into CAMHBT containing 50 mg L^{-1} Ca^{2+}, and 1/100 in MH containing 50 mg L^{-1} Ca^{2+}, and 8 mg L^{-1} daptomycin. All suspected
679 daptomycin-resistant colonies were confirmed using a daptomycin BMD MIC as before.
680 To determine which mutations were present in the rifamycin-resistant isolates, a random
681 selection of 300 colonies, 150 from rifaximin treated mice and 150 from rifampicin treated
682 mice, were sampled for WGS as described above.

683 **Analysis of VREfm isolates from patients receiving rifaximin.**

684 To examine the potential association of rifaximin use in humans and the presence of
685 daptomycin-resistant VREfm strains, we analysed VREfm collected between 2018 and 2021
686 from a single hospital institution in Melbourne. These isolates underwent WGS and
687 daptomycin and rifampicin susceptibility testing as before. Isolates were stratified according
688 to whether the patient received rifaximin within 1 month of VREfm isolation or remained
689 rifaximin free prior to isolate collection. The majority (80%) of isolates were routine screening
690 samples. This included 50 VREfm isolates from patients receiving or previously receiving
691 rifaximin at time of isolation, which were randomly matched to 50 VREfm isolates from
692 patients not receiving rifaximin administration. All isolates were collected within the same
693 time frame. The VREfm isolates were visualised in a maximum-likelihood phylogenetic tree as
694 before, using a core-SNP alignment of 12,430 sites. Isolate MLST was defined with the mlst
695 tool and mutations in RpoB were determined using Snippy
696 (https://github.com/tseemann/snippy) (v4.4.5) as described.

697 **Data visualisation and statistics**

698 All figures were generated in R (v4.0.3, https://www.r-project.org/) using tidyverse (v.1.3.1),
699 patchwork (v.1.1.1), and ggnewscale (v.0.4.5). Statistical analyses were performed using R
700 (v4.0.3, https://www.r-project.org/) and GraphPad Prism (v9.3.1) software packages. Specific
701 tests are given together with each result in the text.

702 **Ethics approval**

703 Ethical approval for analysis of patient data was received from the University of Melbourne
704 Human Research Ethics Committee (study number 1954615.3).

705 **Competing Interests**

706 The authors declare no competing interests.

707 **Acknowledgements**

708 This work was supported by the National Health and Medical Research Council (NHMRC) of
709 Australia (GNT1185213 and GNT1160745). BPH is supported by an NHMRC Investigator Grant
710 (GNT1196103). JCK is supported by an NHMRC Early Career Fellowship (GNT1142613). AMT
711 and NLS are supported by an Australian Government Research Training Program scholarship.
712 The Controlling Superbugs study was supported by the Melbourne Genomics Health Alliance
713 (funded by the State Government of Victoria, Department of Health and Human Services, and
714 the 10 member organizations).

715 **Author Contributions**

716 GPC, BPH, and CLG conceived and planned the experiments. AMT, LL, IRM, DLI, SD, and GPC
717 performed the planned experiments. JCK provided access to necessary patient metadata and
718 clinical VREfm isolates that were used in the study. JYHL, NLS, TPS, and JCK provided critical
719 clinical or bioinformatic insights for the study. AMT, CLG, and GPC co-wrote the manuscript
720 with critical feedback and input from all authors.

721 **Corresponding Authors**

Correspondence to Glen Carter or Benjamin Howden.

Data Availability

The data presented in the study are deposited under Bioprojects PRJNA565795, PRJNA433676, PRJNA856406, and PRJNA856406.

727 **References**

728 1. Murray, C. J. *et al.* Global burden of bacterial antimicrobial resistance in 2019: a
729 systematic analysis. *The Lancet* **399**, 629–655 (2022).
730 2. Bylicka-Szczepanowska, E. & Korzeniewski, K. Asymptomatic Malaria Infections in the
731 Time of COVID-19 Pandemic: Experience from the Central African Republic. *Int. J. Environ.*
732 *Res. Public. Health* **19**, 3544 (2022).
733 3. Global HIV & AIDS statistics — Fact sheet. https://www.unaids.org/en/resources/fact-
734 sheet.
735 4. GBD 2019 Collaborators. Global mortality from dementia: Application of a new method
736 and results from the Global Burden of Disease Study 2019. *Alzheimers Dement. N. Y. N* **7**,
737 e12200 (2021).
738 5. Arias, C. A. & Murray, B. E. The rise of the *Enterococcus*: beyond vancomycin resistance.
739 *Nat. Rev. Microbiol.* **10**, 266–278 (2012).
740 6. Top, J., Willems, R. & Bonten, M. Emergence of CC17 *Enterococcus faecium*: from
741 commensal to hospital-adapted pathogen. *FEMS Immunol. Med. Microbiol.* **52**, 297–308
742 (2008).
743 7. Arthur, M. & Courvalin, P. Genetics and mechanisms of glycopeptide resistance in
744 enterococci. *Antimicrob. Agents Chemother.* **37**, 1563–1571 (1993).
745 8. Tacconelli, E. *et al.* Discovery, research, and development of new antibiotics: the WHO
746 priority list of antibiotic-resistant bacteria and tuberculosis. *Lancet Infect. Dis.* **18**, 318–
747 327 (2018).
748 9. Montero, C. I., Stock, F. & Murray, P. R. Mechanisms of Resistance to Daptomycin in
749 *Enterococcus faecium*. *Antimicrob. Agents Chemother.* (2008) doi:10.1128/AAC.00774-07.

750 10. Greene, M. H. *et al.* Risk Factors and Outcomes Associated With Acquisition of
751 Daptomycin and Linezolid–Nonsusceptible Vancomycin-Resistant *Enterococcus*. *Open*
752 *Forum Infect. Dis.* **5**, ofy185 (2018).
753 11. Egli, A. *et al.* Association of daptomycin use with resistance development in
754 *Enterococcus faecium* bacteraemia—a 7-year individual and population-based analysis.
755 *Clin. Microbiol. Infect.* **23**, 118.e1-118.e7 (2017).
756 12. Diaz, L. *et al.* Whole-Genome Analyses of *Enterococcus faecium* Isolates with Diverse
757 Daptomycin MICs. *Antimicrob. Agents Chemother.* (2014).
758 13. Lellek, H. *et al.* Emergence of daptomycin non-susceptibility in colonizing
759 vancomycin-resistant *Enterococcus faecium* isolates during daptomycin therapy. *Int. J.*
760 *Med. Microbiol.* **305**, 902–909 (2015).
761 14. Kelesidis, T., Tewhey, R. & Humphries, R. M. Evolution of high-level daptomycin
762 resistance in *Enterococcus faecium* during daptomycin therapy is associated with limited
763 mutations in the bacterial genome. *J. Antimicrob. Chemother.* **68**, 1926–1928 (2013).
764 15. Werth, B. J. *et al.* Defining Daptomycin Resistance Prevention Exposures in
765 Vancomycin-Resistant *Enterococcus faecium* and *E. faecalis*. *Antimicrob. Agents*
766 *Chemother.* **58**, 5253–5261 (2014).
767 16. Turner, A. M., Lee, J. Y. H., Gorrie, C. L., Howden, B. P. & Carter, G. P. Genomic
768 Insights Into Last-Line Antimicrobial Resistance in Multidrug-Resistant *Staphylococcus* and
769 Vancomycin-Resistant *Enterococcus*. *Front. Microbiol.* **12**, (2021).
770 17. Li, L. *et al.* Daptomycin Resistance Occurs Predominantly in vanA-Type Vancomycin-
771 Resistant *Enterococcus faecium* in Australasia and Is Associated With Heterogeneous and
772 Novel Mutations. *Front. Microbiol.* **12**, 749935 (2021).

773 18. Bass, N. M. *et al.* Rifaximin Treatment in Hepatic Encephalopathy. *N. Engl. J. Med.*
774 **362**, 1071–1081 (2010).
775 19. Shayto, R. H., Abou Mrad, R. & Sharara, A. I. Use of rifaximin in gastrointestinal and
776 liver diseases. *World J. Gastroenterol.* **22**, 6638–6651 (2016).
777 20. Sherry, N. L. *et al.* Pilot study of a combined genomic and epidemiologic surveillance
778 program for hospital-acquired multidrug-resistant pathogens across multiple hospital
779 networks in Australia. *Infect. Control Hosp. Epidemiol.* **42**, 573–581 (2021).
780 21. Gorrie, C. L. *et al.* Key parameters for genomics-based real-time detection and
781 tracking of multidrug-resistant bacteria: a systematic analysis. *Lancet Microbe* **2**, e575–
782 e583 (2021).
783 22. Miller, W. R., Bayer, A. S. & Arias, C. A. Mechanism of Action and Resistance to
784 Daptomycin in *Staphylococcus aureus* and Enterococci. *Cold Spring Harb. Perspect. Med.*
785 **6**, a026997 (2016).
786 23. Prater, A. G. *et al.* Environment Shapes the Accessible Daptomycin Resistance
787 Mechanisms in *Enterococcus faecium. Antimicrob. Agents Chemother.* **63**, e00790-19.
788 24. Bæk, K. T. *et al.* Stepwise Decrease in Daptomycin Susceptibility in Clinical
789 *Staphylococcus aureus* Isolates Associated with an Initial Mutation in *rpoB* and a
790 Compensatory Inactivation of the clpX Gene. *Antimicrob. Agents Chemother.* (2015).
791 25. Cui, L. *et al.* An RpoB Mutation Confers Dual Heteroresistance to Daptomycin and
792 Vancomycin in *Staphylococcus aureus*. *Antimicrob. Agents Chemother.* (2010)
793 doi:10.1128/AAC.00437-10.
794 26. Goldstein, B. P. Resistance to rifampicin: a review. *J. Antibiot. (Tokyo)* **67**, 625–630
795 (2014).

796 27. Rios, R. *et al.* Genomic Epidemiology of Vancomycin-Resistant *Enterococcus faecium*
797 (VREfm) in Latin America: Revisiting The Global VRE Population Structure. *Sci. Rep.* **10**,
798 5636 (2020).
799 28. Duchêne, S. *et al.* Genome-scale rates of evolutionary change in bacteria. *Microb.*
800 *Genomics* **2**, e000094 (2016).
801 29. Lebreton, F. *et al.* Emergence of Epidemic Multidrug-Resistant *Enterococcus faecium*
802 from Animal and Commensal Strains. *mBio* **4**, e00534-13.
803 30. Raven, K. E. *et al.* A decade of genomic history for healthcare-associated
804 *Enterococcus faecium* in the United Kingdom and Ireland. *Genome Res.* **26**, 1388–1396
805 (2016).
806 31. Goel, A., Rahim, U., Nguyen, L. H., Stave, C. & Nguyen, M. H. Systematic review with
807 meta-analysis: rifaximin for the prophylaxis of spontaneous bacterial peritonitis. *Aliment.*
808 *Pharmacol. Ther.* **46**, 1029–1036 (2017).
809 32. Lee, R. A. *et al.* Daptomycin-Resistant *Enterococcus* Bacteremia Is Associated With
810 Prior Daptomycin Use and Increased Mortality After Liver Transplantation. *Open Forum*
811 *Infect. Dis.* **9**, ofab659 (2022).
812 33. Morley, V. J. *et al.* An adjunctive therapy administered with an antibiotic prevents
813 enrichment of antibiotic-resistant clones of a colonizing opportunistic pathogen. *eLife* **9**,
814 e58147 (2020).
815 34. Bender, J. K. *et al.* Update on prevalence and mechanisms of resistance to linezolid,
816 tigecycline and daptomycin in enterococci in Europe: Towards a common nomenclature.
817 *Drug Resist. Updat.* **40**, 25–39 (2018).

818 35. Tran, T. T. *et al.* Whole-Genome Analysis of a Daptomycin-Susceptible *Enterococcus*
819 *faecium* Strain and Its Daptomycin-Resistant Variant Arising during Therapy. *Antimicrob.*
820 *Agents Chemother.* **57**, 261–268 (2013).
821 36. Zaw, M. T., Emran, N. A. & Lin, Z. Mutations inside rifampicin-resistance determining
822 region of *rpoB* gene associated with rifampicin-resistance in *Mycobacterium tuberculosis*.
823 *J. Infect. Public Health* **11**, 605–610 (2018).
824 37. Lee, J. Y. H. *et al.* Global spread of three multidrug-resistant lineages of
825 *Staphylococcus epidermidis*. *Nat. Microbiol.* **3**, 1175–1185 (2018).
826 38. Guérillot, R. *et al.* Convergent Evolution Driven by Rifampin Exacerbates the Global
827 Burden of Drug-Resistant *Staphylococcus aureus*. *mSphere* **3**, e00550-17.
828 39. Albarillo, F. S., Medina, R. E., Joyce, C. S., Darji, H. & Santarossa, M. Daptomycin-
829 resistant VRE infections: a descriptive analysis at a single academic centre. *Infect. Dis.* **53**,
830 393–395 (2021).
831 40. Teillant, A., Gandra, S., Barter, D., Morgan, D. J. & Laxminarayan, R. Potential burden
832 of antibiotic resistance on surgery and cancer chemotherapy antibiotic prophylaxis in the
833 USA: a literature review and modelling study. *Lancet Infect. Dis.* **15**, 1429–1437 (2015).
834 41. Berríos-Torres, S. I. *et al.* Activity of Commonly Used Antimicrobial Prophylaxis
835 Regimens against Pathogens Causing Coronary Artery Bypass Graft and Arthroplasty
836 Surgical Site Infections in the United States, 2006–2009. *Infect. Control Hosp. Epidemiol.*
837 **35**, 231–239 (2014).
838 42. Dyar, O. J., Huttner, B., Schouten, J. & Pulcini, C. What is antimicrobial stewardship?
839 *Clin. Microbiol. Infect.* **23**, 793–798 (2017).

840 43. Lee, R. S. *et al.* The changing landscape of vancomycin-resistant *Enterococcus*
841 *faecium* in Australia: a population-level genomic study. *J. Antimicrob. Chemother.* **73**,
842 3268–3278 (2018).
843 44. Snyder, E. E. *et al.* PATRIC: The VBI PathoSystems Resource Integration Center.
844 *Nucleic Acids Res.* **35**, D401–D406 (2007).
845 45. Wood, D. E., Lu, J. & Langmead, B. Improved metagenomic analysis with Kraken 2.
846 *Genome Biol.* **20**, 257 (2019).
847 46. Humphries, R. M. The New, New Daptomycin Breakpoint for *Enterococcus* spp. *J.*
848 *Clin. Microbiol.* **57**, e00600-19.
849 47. Lam, M. M. *et al.* Comparative analysis of the complete genome of an epidemic
850 hospital sequence type 203 clone of vancomycin-resistant *Enterococcus faecium*. *BMC*
851 *Genomics* **14**, 595 (2013).
852 48. Bankevich, A. *et al.* SPAdes: A New Genome Assembly Algorithm and Its Applications
853 to Single-Cell Sequencing. *J. Comput. Biol.* **19**, 455–477 (2012).
854 49. Schliep, K. P. phangorn: phylogenetic analysis in R. *Bioinformatics* **27**, 592–593
855 (2011).
856 50. Paradis, E. & Schliep, K. ape 5.0: an environment for modern phylogenetics and
857 evolutionary analyses in R. *Bioinformatics* **35**, 526–528 (2019).
858 51. Yu, G., Smith, D. K., Zhu, H., Guan, Y. & Lam, T. T.-Y. ggtree: an r package for
859 visualization and annotation of phylogenetic trees with their covariates and other
860 associated data. *Methods Ecol. Evol.* **8**, 28–36 (2017).
861 52. Crispell, J., Balaz, D. & Gordon, S. V. HomoplasyFinder: a simple tool to identify
862 homoplasies on a phylogeny. *Microb. Genomics* **5**, e000245 (2019).

863 53. Lees, J. A., Galardini, M., Bentley, S. D., Weiser, J. N. & Corander, J. pyseer: a
864 comprehensive tool for microbial pangenome-wide association studies. *Bioinformatics*
865 **34**, 4310–4312 (2018).
866 54. de Been, M. *et al.* Core Genome Multilocus Sequence Typing Scheme for High-
867 Resolution Typing of *Enterococcus faecium*. *J. Clin. Microbiol.* **53**, 3788–3797 (2015).
868 55. Croucher, N. J. *et al.* Rapid phylogenetic analysis of large samples of recombinant
869 bacterial whole genome sequences using Gubbins. *Nucleic Acids Res.* **43**, e15 (2015).
870 56. Nguyen, L.-T., Schmidt, H. A., von Haeseler, A. & Minh, B. Q. IQ-TREE: A Fast and
871 Effective Stochastic Algorithm for Estimating Maximum-Likelihood Phylogenies. *Mol. Biol.*
872 *Evol.* **32**, 268–274 (2015).
873 57. Rambaut, A., Lam, T. T., Max Carvalho, L. & Pybus, O. G. Exploring the temporal
874 structure of heterochronous sequences using TempEst (formerly Path-O-Gen). *Virus Evol.*
875 **2**, vew007 (2016).
876 58. Suchard, M. A. *et al.* Bayesian phylogenetic and phylodynamic data integration using
877 BEAST 1.10. *Virus Evol.* **4**, vey016 (2018).
878 59. Minin, V. N. & Suchard, M. A. Counting labeled transitions in continuous-time
879 Markov models of evolution. *J. Math. Biol.* **56**, 391–412 (2008).
880 60. Minin, V. N. & Suchard, M. A. Fast, accurate and simulation-free stochastic mapping.
881 *Philos. Trans. R. Soc. B Biol. Sci.* **363**, 3985–3995 (2008).
882 61. Monk, I. R., Tree, J. J., Howden, B. P., Stinear, T. P. & Foster, T. J. Complete Bypass of
883 Restriction Systems for Major *Staphylococcus aureus* Lineages. *mBio* **6**, e00308-15.
884 62. Zhang, Y., Werling, U. & Edelmann, W. Seamless Ligation Cloning Extract (SLiCE)
885 Cloning Method. in *DNA Cloning and Assembly Methods* (eds. Valla, S. & Lale, R.) 235–244
886 (Humana Press, 2014). doi:10.1007/978-1-62703-764-8_16.

887 63. Pidot, S. J. *et al.* Increasing tolerance of hospital *Enterococcus faecium* to handwash
888 alcohols. *Sci. Transl. Med.* **10**, eaar6115 (2018).
889 64. Nair, A. B. & Jacob, S. A simple practice guide for dose conversion between animals
890 and human. *J. Basic Clin. Pharm.* **7**, 27–31 (2016).
891 65. Heine, H. S., Bassett, J., Miller, L., Purcell, B. K. & Byrne, W. R. Efficacy of Daptomycin
892 against *Bacillus anthracis* in a Murine Model of Anthrax Spore Inhalation. *Antimicrob.*
893 *Agents Chemother.* **54**, 4471–4473 (2010).
894
895

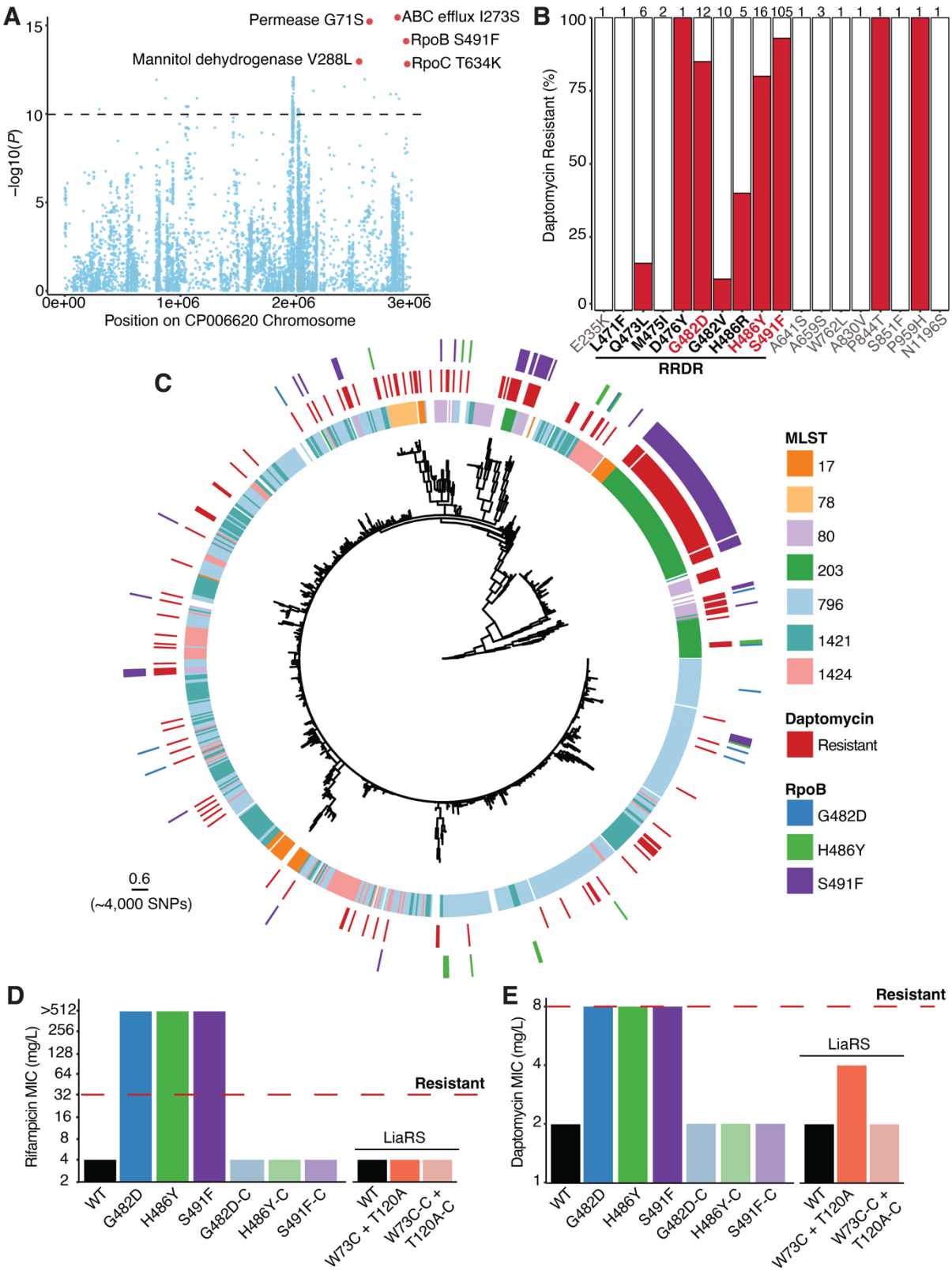
A
Permease G71S
ABC efflux I273S
RpoB S491F
RpoC T634K
Mannitol dehydrogenase V288L
−log10(P)
Position on CP006620 Chromosome
B
Daptomycin Resistant (%)
E235K
L471F
Q473L
M475I
D476Y
G482D
G482V
H486R
H486Y
S491F
A641S
A659S
W762L
A830V
P844T
S851F
P959H
N1196S
RRDR
C
MLST
17
78
80
203
796
1421
1424
Daptomycin
Resistant
RpoB
G482D
H486Y
S491F
0.6
(~4,000 SNPs)
D
Rifampicin MIC (mg/L)
Resistant
LiaRS
WT
G482D
H486Y
S491F
G482D-C
H486Y-C
S491F-C
W73C + T120A
W73C-C + T120A-C
E
Daptomycin MIC (mg/L)
Resistant
LiaRS

896

897 **Figure 1. A.** Manhattan plot of 10,530 variants, displayed by position on the reference
898 genome and significance association with daptomycin resistance (univariate analysis using a
899 linear mixed model). The dashed line shows the Bonferroni-corrected significance threshold.
900 **B.** Percentage of daptomycin-resistant strains for each mutation within RpoB. The mutations
901 within the rifampicin resistance determining region (RRDR) are shown in bold. Mutations
902 coloured in red were associated with daptomycin resistance. The total number of strains
903 containing each mutation is shown above each bar. **C.** Maximum-likelihood core-SNP-based
904 phylogeny of clinical VREfm (n=1000) inferred from 6,574 SNPs, demonstrating the presence
905 of RpoB mutations in daptomycin-resistant isolates. Overlaid are the results of *in silico* multi-
906 locus sequence type (MLST), daptomycin phenotypic testing, and mutations associated with
907 daptomycin resistance in RpoB. In the first circle, ST is not shown for uncommon STs (n≤5).
908 The scale bar indicates number of nucleotide substitutions per site (top), with an
909 approximation of SNP distance (in parentheses). **D.** Rifampicin susceptibility testing results
910 for the WT, isogenic *rpoB* and *liaRS* isogenic mutants and complement strains (designated
911 with -C) (n=3). **E.** Daptomycin susceptibility testing results for the WT, *rpoB* and *liaRS* isogenic
912 mutants and complement strains (designated with -C) (n=3). The median MIC for each strain
913 is shown.

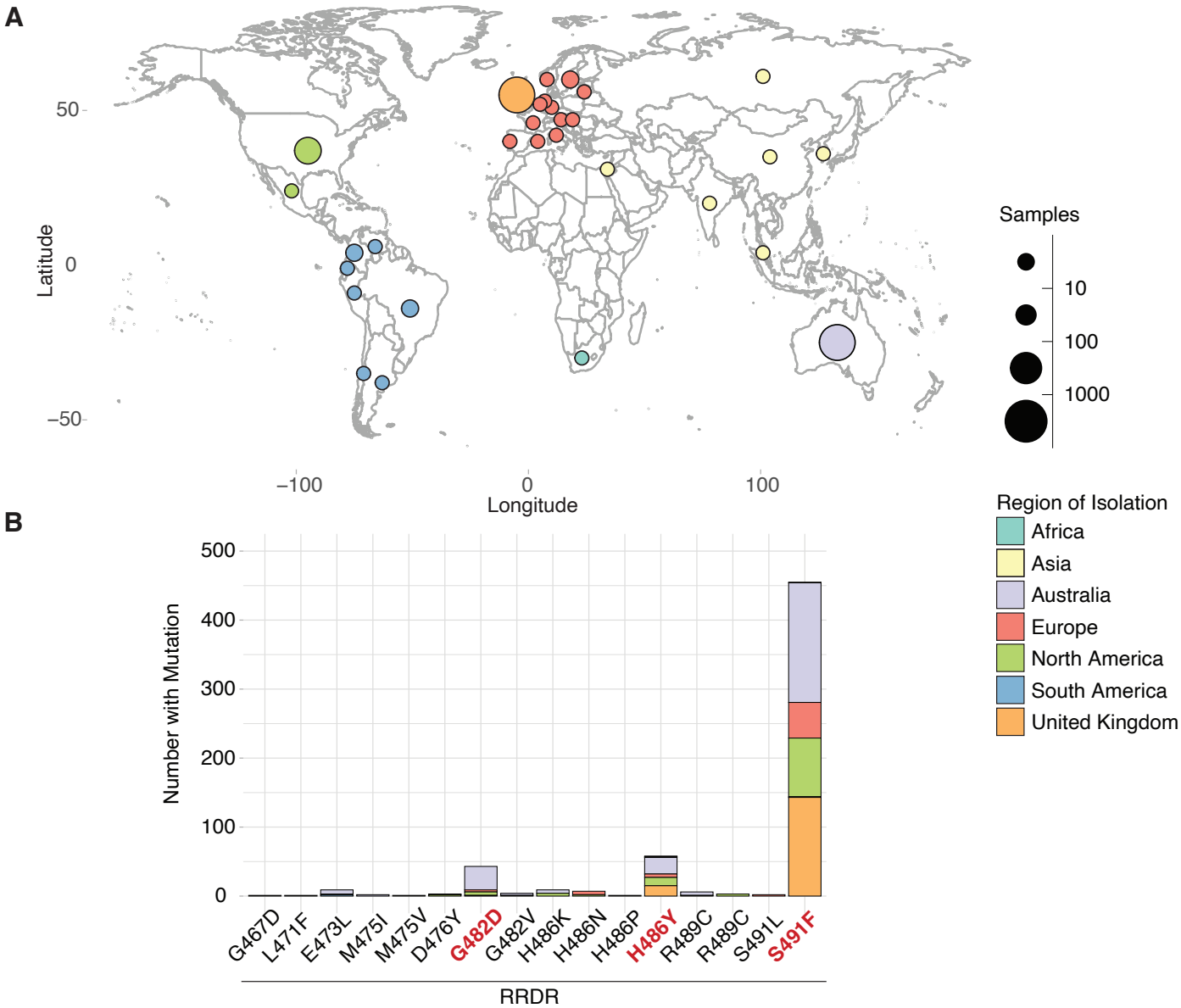
A
50
0
−50
Latitude
−100
0
100
Longitude
Samples
10
100
1000
Region of Isolation
Africa
Asia
Australia
Europe
North America
South America
United Kingdom
B
500
400
300
200
100
0
Number with Mutation
G467D
L471F
E473L
M475I
M475V
D476Y
G482D
G482V
H486K
H486N
H486P
H486V
R489C
R489C
S491L
S491F
RRDR

914

915 **Figure 2. A.** Map of 4,476 VREfm genomes included in this study. Circle size corresponds to
916 total number of genomes (binned into categories), and colour corresponds to region of
917 isolation. Country coordinates used are the country centroid position. Map was generated in
918 R using ggplot2. **B.** The frequency of various RpoB mutations within the rifampicin resistance
919 determining region (RRDR) in 4,476 VREfm genomes, sampled from 43 MLSTs. Bars are
920 coloured by the number of isolates from each region of isolation containing the mutation. The
921 identified daptomycin resistance associated mutations are coloured in red.

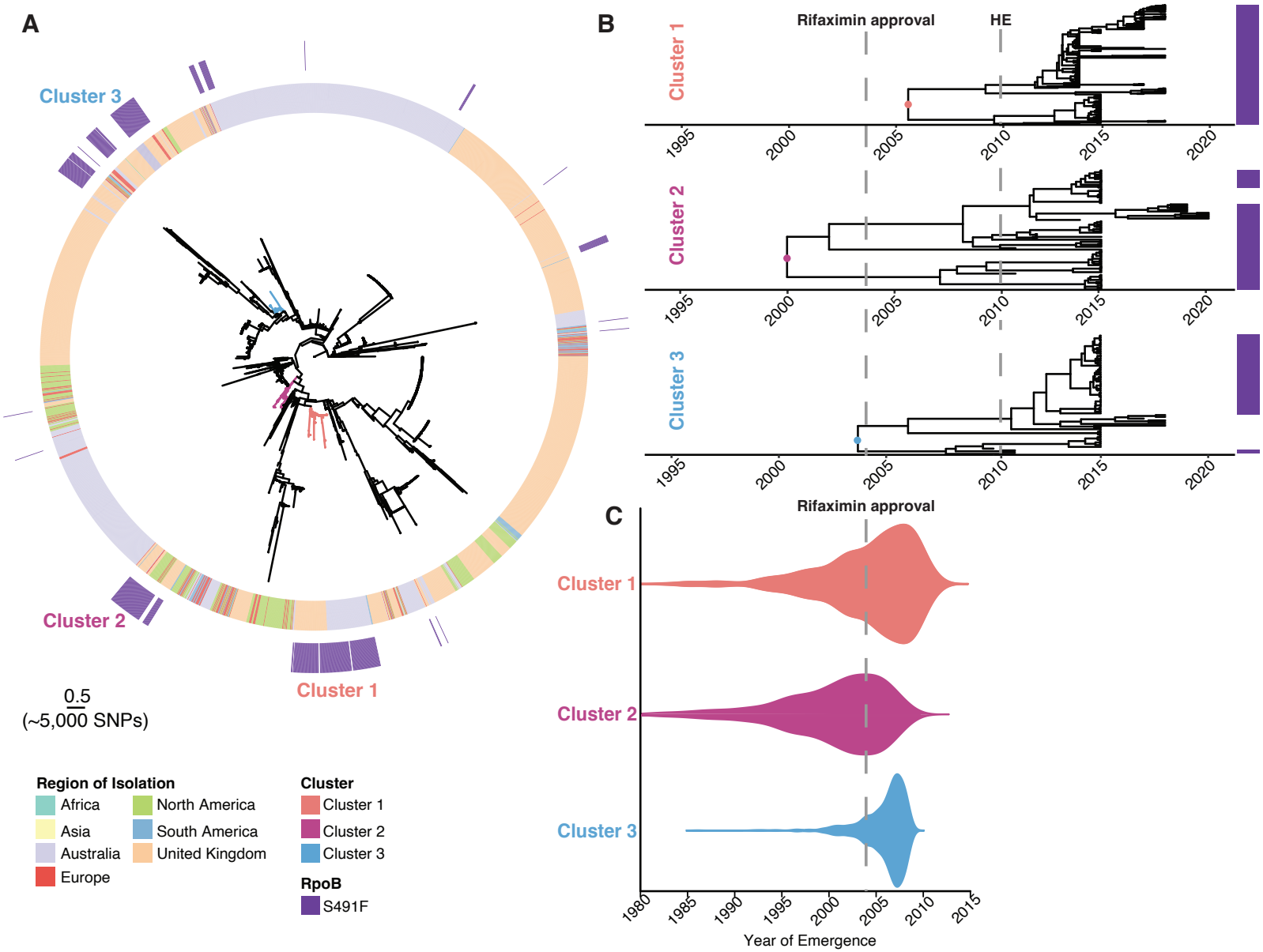
A
Cluster 3
Cluster 2
Cluster 1
0.5
(~5,000 SNPs)
Region of Isolation
Africa
Asia
Australia
Europe
North America
South America
United Kingdom
Cluster
Cluster 1
Cluster 2
Cluster 3
RpoB
S491F
B
Rifaximin approval
HE
Cluster 1
Cluster 2
Cluster 3
1995
2000
2005
2010
2015
2020
C
Rifaximin approval
Cluster 1
Cluster 2
Cluster 3
1980
1985
1990
1995
2000
2005
2010
2015
Year of Emergence

922

923 **Figure 3. A.** Maximum-likelihood, core-SNP-based phylogeny for 4,476 VREfm inferred from
924 9,277 core-genome SNPs, demonstrating the presence of the S491F RpoB mutation in
925 international VREfm. Overlaid is the region of isolation for each strain and the presence of the
926 S491F mutation. The coloured branches indicate the three VREfm clusters identified with
927 cgMLST used as input for Bayesian evolutionary analyses. The scale bar indicates number of
928 nucleotide substitutions per site (top), with an approximation of SNP distance (in
929 parentheses). **B.** Bayesian phylodynamic analyses showing the maximum-clade credibility
930 (MCC) trees of the three VREfm clusters with the timing of emergence for each lineage.
931 Cluster 1 (n=219) was inferred from a core alignment of 1,869,554 bp containing 329 SNP
932 sites; Cluster 2 (n=85) was inferred from an alignment of 1,524,024 bp containing 541 SNP
933 sites; and Cluster 3 (n=68) was inferred from an alignment of 1,860,780 bp containing 764
934 SNP sites. The time in years is given on the *x* axis. The presence of the S491F RpoB trait for
935 each isolate is shown in purple. Overlaid onto the MCC trees is the first instance of FDA
936 approval for rifaximin (2004) and for hepatic encephalopathy (HE) (2010). **C.** Violin plots for
937 the most recent common ancestor (MCRA) for each cluster, representing when the RpoB
938 S491F mutation first emerged, with 95% HPD intervals. Overlaid onto violin plots is the FDA
939 approval date for rifaximin (2004).

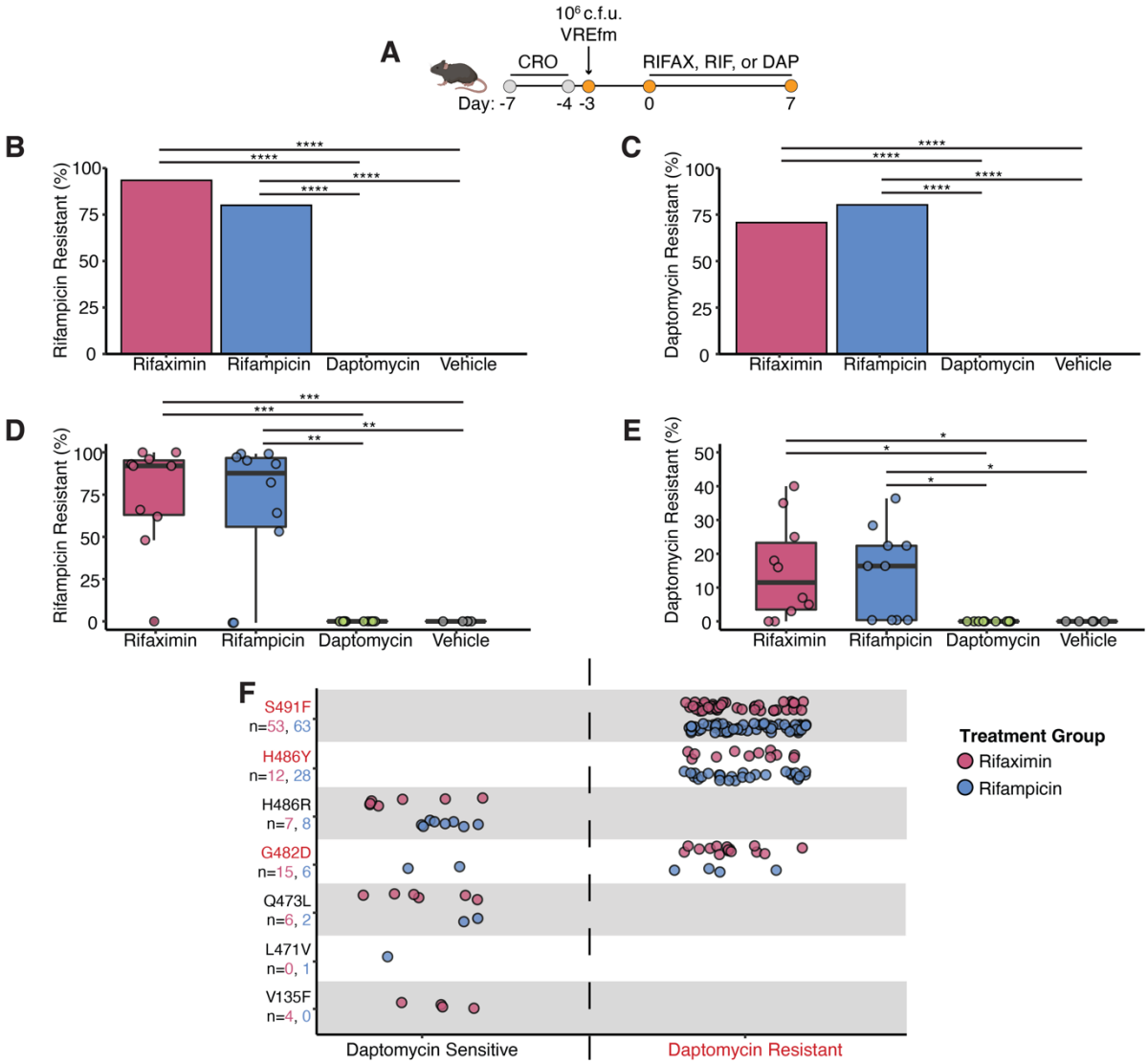
A
10⁶ c.f.u.
VREfm
CRO
RIFAX, RIF, or DAP
Day: -7
-4 -3
0
7
B
Rifampicin Resistant (%)
Rifaximin
Rifampicin
Daptomycin
Vehicle
C
Daptomycin Resistant (%)
D
E
F
S491F
n=53, 63
H486Y
n=12, 28
H486R
n=7, 8
G482D
n=15, 6
Q473L
n=6, 2
L471V
n=0, 1
V135F
n=4, 0
Daptomycin Sensitive
Daptomycin Resistant
Treatment Group
Rifaximin
Rifampicin

940

941 **Figure 4. A.** Timeline of the mouse experiment. VREfm-colonised mice (n=5 for vehicle, n=10
942 for rifampicin, n=10 for rifaximin, n=10 for daptomycin) received a human-equivalent dose of
943 vehicle, rifampicin, or rifaximin (twice per day for rifaximin) for 7 days by oral gavage or
944 subcutaneous injection with daptomycin for 7 days. CRO=ceftriaxone; DAP=daptomycin;
945 RIFAX=rifaximin; RIF=rifampicin. Figure to scale. **B.** Percentage of total mice with rifampicin-
946 resistant VREfm strains **C.** or daptomycin-resistant VREfm strains after 7 days of antibiotic
947 treatment. **D.** Percentage of VREfm from each mouse (n=50 colonies per mouse) that were
948 resistant to rifampicin **E.** or daptomycin after 7 days of antibiotic treatment. Points represent
949 an individual mouse. Percentage was calculated from rifampicin or daptomycin MIC values
950 (either resistant or susceptible) from 50 VREfm colonies isolated from each mouse. Boxes
951 represent the median and interquartile range for each group. **F.** Overview of the RpoB
952 mutations identified in the rifampicin-resistant colonies. Each point represents a single
953 colony. Isolates are separated by each RpoB mutation and grouped into either daptomycin-
954 susceptible or daptomycin-resistant. The RpoB mutations coloured in red had an association
955 with daptomycin resistance. n values represent the number of isolates containing each
956 mutation for rifaximin and rifampicin, respectively. *$P < 0.05$, **$P < 0.01$, ***$P < 0.001$,
957 ****$P<0.0001$; unpaired *t*-test (vehicle versus rifampicin or vehicle versus rifaximin and
958 rifampicin verses daptomycin or rifaximin verses daptomycin).

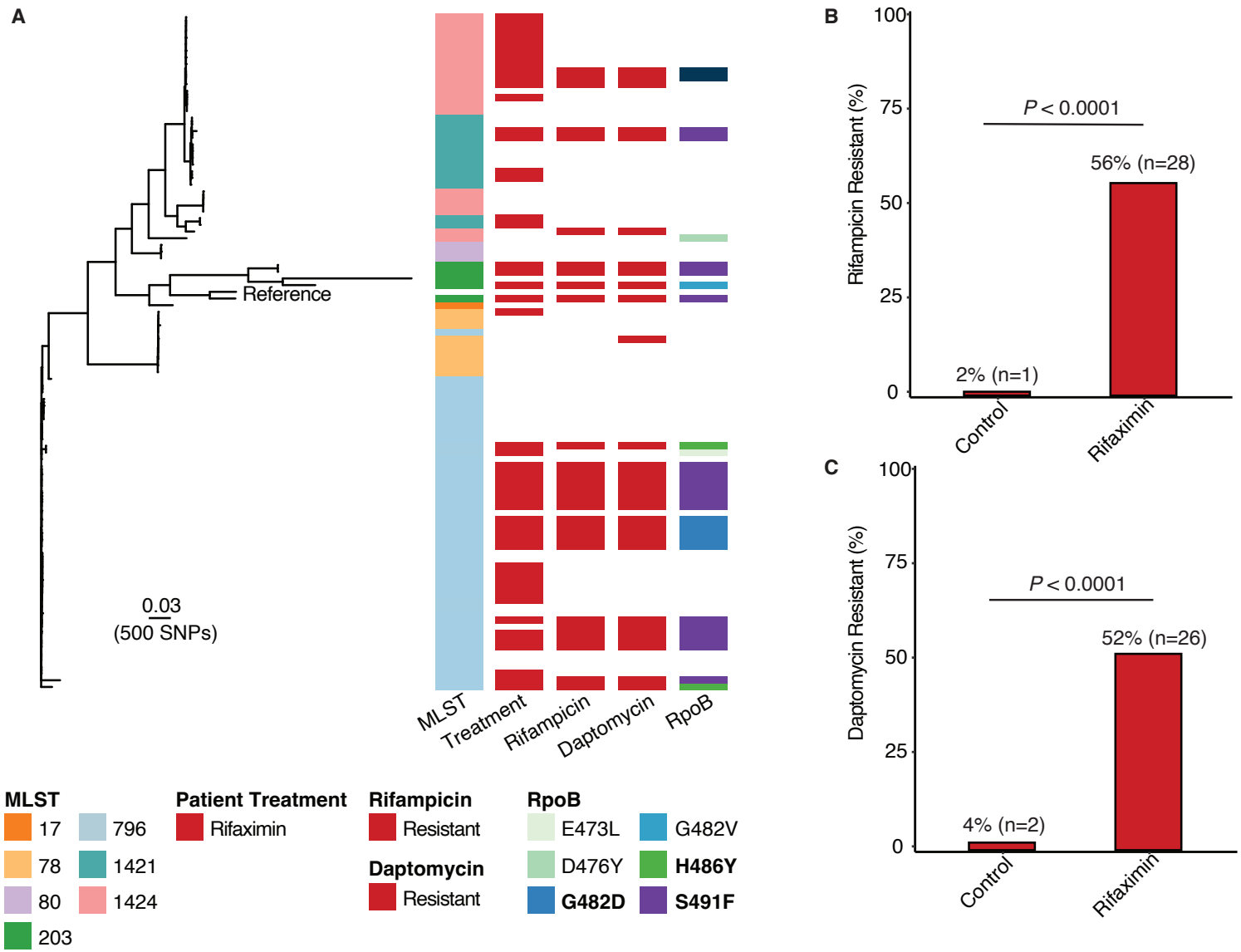
A
Reference
0.03
(500 SNPs)
MLST
Treatment
Rifampicin
Daptomycin
RpoB
MLST
17
78
80
203
796
1421
1424
Patient Treatment
Rifaximin
Rifampicin
Resistant
Daptomycin
Resistant
RpoB
E473L
D476Y
G482D
G482V
H486Y
S491F
B
Rifampicin Resistant (%)
100
75
50
25
0
P < 0.0001
56% (n=28)
2% (n=1)
Control
Rifaximin
C
Daptomycin Resistant (%)
100
75
50
25
0
P < 0.0001
52% (n=26)
4% (n=2)
Control
Rifaximin

959

960 **Figure 5. A.** Maximum-likelihood core-SNP-based phylogeny of clinical VREfm (n=100)
961 inferred from 12,430 SNPs. Overlaid is the results of *in silico* MLST, rifaximin treatment group,
962 rifampicin phenotypic testing, daptomycin phenotypic testing, and mutations in RpoB.
963 Mutations associated with daptomycin resistance are bolded. The scale bar indicates number
964 of nucleotide substitutions per site (top), with an approximation of SNP distance (in
965 parentheses). **B.** Rifampicin susceptibility data for clinical VREfm (n=50 per group). Red bars
966 represent percent of rifampicin-resistant isolates. A Fisher's exact test comparing the
967 percentage of rifampicin resistance in the control versus rifaximin, $P < 0.0001$. **C.** Daptomycin
968 susceptibility data for clinical VREfm (n=50 per group). Red bars represent percent of
969 daptomycin-resistant isolates. A Fisher's exact test comparing the percentage of daptomycin
970 resistance in the control versus rifaximin, $P < 0.0001$.